Journal of Biomedical Optics

BiomedicalOptics.SPIEDigitalLibrary.org

Statistical analysis of polarization-inhomogeneous Fourier spectra of laser radiation scattered by human skin in the tasks of differentiation of benign and malignant formations

Alexander G. Ushenko
Alexander V. Dubolazov
Vladimir A. Ushenko
Olga Y. Novakovskaya

SPIE.

Statistical analysis of polarization-inhomogeneous Fourier spectra of laser radiation scattered by human skin in the tasks of differentiation of benign and malignant formations

Alexander G. Ushenko,[a] Alexander V. Dubolazov,[a,*] Vladimir A. Ushenko,[b] and Olga Y. Novakovskaya[c]
[a]Chernivtsi National University, Optics and Publishing Department, 2 Kotsiubynskyi Street, Chernivtsi, Ukraine
[b]Chernivtsi National University, Correlation Optics Department, 2 Kotsiubynskyi Street, Chernivtsi, Ukraine
[c]Bukovinian State Medical University, Department of Medical Physics and Biological Informatics, 2 Theatral Square, Chernivtsi, Ukraine

Abstract. The optical model of formation of polarization structure of laser radiation scattered by polycrystalline networks of human skin in Fourier plane was elaborated. The results of investigation of the values of statistical (statistical moments of the 1st to 4th order) parameters of polarization-inhomogeneous images of skin surface in Fourier plane were presented. The diagnostic criteria of pathological process in human skin and its severity degree differentiation were determined. [DOI: 10.1117/1.JBO.21.7.071110]

Keywords: polarization; Fourier optics; optical anisotropy; biological tissue; diagnostics.

Paper 150647SSRR received Oct. 13, 2015; accepted for publication Feb. 9, 2016; published online Mar. 8, 2016.

1 Introduction

Investigations *in vitro* prevail among various optical and physical techniques of diagnostics of structure and properties of biological objects.[1–11] Particularly, laser polarimetry of microscopic images of polycrystalline protein networks was formed as a separate approach in the study of optically anisotropic component of histological sections of biopsy of different biological tissues.[12–19] The analytical methods used in laser polarimetry are based on the approximation of linear birefringence of biological tissues. On the basis of the above-mentioned approach there has been found an interconnection between the set of statistic moments of the 1st to 4th orders, which characterize the azimuth and ellipticity distributions of laser images, and the physiological state of biological tissue layer. As the result, the method of polarization mapping and the successful diagnostics of oncological (malignant) changes of human biological tissues have been elaborated. At the same time, such diagnostics requires a traumatic and not always safe procedure of biopsy. This fact limits the possibility of screening investigations in clinical practice.

In order to extend the functional possibilities of noninvasive (optical) and accurate (comparable with histological methods) oncological diagnostics, the application of polarization mapping of biological tissues *in vivo* is topical. In this situation, the obtaining of convenient microscopic images is complicated due to the high level of diffuse background. Fourier polarimetry of biological tissue can be used as an alternative approach.[20] Such a method allows the ability to concentrate the reflected by biological tissue radiation and perform the polarization mapping of obtained Fourier spectra. At the same time, polarization structure of Fourier spectra of object fields of biological tissues *in vivo* is practically unexplored.

This research is aimed at investigation of efficiency of optical differentiation of benign (adenoma) and precancer (keratoma) changes of human skin utilizing the statistical analysis of polarization-inhomogeneous Fourier spectra of scattered laser radiation.

2 Basic Analytical Relations

Let us consider the process of forming a polarization-inhomogeneous Fourier spectra of the reflected laser radiation by human skin. In Refs. 12,16–18 what has been proposed and experimentally proved is the model of amorphous-crystalline structure of planar layers of main types of biological tissues: connective, muscular, epithelial, and nervous. Within the limits of such an approach, it has been shown that the following matrix operator can characterize the optical properties of polycrystalline networks anisotropy[20]

$$D=\left\|\begin{matrix} d_{11}(\rho,\phi,\theta) & d_{12}(\rho,\phi,\theta) \\ d_{21}(\rho,\phi,\theta) & d_{22}(\rho,\phi,\theta) \end{matrix}\right\|= \\ =\left\|\begin{matrix} [\sin^2\rho+\cos^2\rho\,\exp(-i\delta)] & [\cos^2\rho+\sin^2\rho\,\exp(-i\delta)] \\ [\cos^2\rho+\sin^2\rho\,\exp(-i\delta)] & [\cos^2\rho+\sin^2\rho\,\exp(-i\delta)] \end{matrix}\right\| \\ \times\left\|\begin{matrix} \cos\theta & \sin\theta \\ -\sin\theta & \cos\theta \end{matrix}\right\|, \quad (1)$$

where $d_{ik}(\rho,\phi,\theta)$ are Jones-matrix elements, which are determined by the directions of optical axis ρ of collagen fibrils and the values of phase shifts of linear (φ) and circular (θ) birefringence.

In accordance with Eq. (1) the processes of formation of polarization-inhomogeneous laser field of polycrystalline

*Address all correspondence to: Alexander V. Dubolazov, E-mail: dubolazov85@yandex.ru

1083-3668/2016/$25.00

network in the plane of skin surface completely described by the following Jones-matrix equation

$$\begin{pmatrix} E_x e^{i\varphi_x} \\ E_y e^{i\varphi_y} \end{pmatrix} = \begin{Vmatrix} d_{11} & d_{12} \\ d_{21} & d_{22} \end{Vmatrix} \begin{pmatrix} E_{0x} e^{i\varphi_{0x}} \\ E_{0y} e^{i\varphi_{0y}} \end{pmatrix} = \begin{pmatrix} d_{11} E_{0x} e^{i\varphi_{0x}} + d_{12} E_{0y} e^{i\varphi_{0y}} \\ d_{21} E_{0x} e^{i\varphi_{0x}} + d_{22} E_{0y} e^{i\varphi_{0y}} \end{pmatrix}. \quad (2)$$

Here φ_{0x} and φ_{0y}—phases of orthogonal components (E_{0x}, E_{0y}) of the amplitude of laser beam probing skin surface, φ_x and φ_y—phases of orthogonal components E_x, E_y of the of laser field amplitude formed by optically anisotropic collagen networks in the plane of skin surface.

From the Eq. (2) it is possible to determine the trajectory of waves polarization in every point (x, y) of laser image of skin surface

$$\frac{x^2}{E_x^2} - \frac{2xy}{E_x E_y} \cos \Delta\varphi + \frac{y^2}{E_y^2} = \sin^2 \Delta\varphi. \quad (3)$$

Here $\Delta\varphi = \varphi_x - \varphi_y$.

Thus, polarization-inhomogeneous [polarization maps $\alpha(x, y)$, $\beta(x, y)$] image of human skin is formed[18]

$$\alpha(x, y) = 0.5 \arcsin\left[\frac{\sin 2\Psi(x, y)}{\cos \Delta\varphi(x, y)}\right]; \quad (4)$$

$$\beta(x, y) = 0.5 \arctan\left[\frac{\sin \Delta\varphi(x, y)}{\cos 2\Psi(x, y)}\right]; \quad (5)$$

$$\Psi = \arctan \frac{E_y}{E_x}. \quad (6)$$

It should be noted that the relations of Eqs. (1)–(6) satisfactorily describe the process of forming of polarization structure of laser radiation transformed by optically thin layers of skin. Such a scenario can be reached as the result of optical investigations of skin *in vitro*. In the *in vivo* regime, due to the multiple scattering of laser radiation in the surface and subsurface layers of skin, the transformation of polarization structure [Eqs. (4)–(6)] of object field of human skin takes place. The formation of such a polarization-inhomogeneous field in the Fourier plane can be described analytically by forward Fourier transform. Taking into account relations Eq. (2) intensity, azimuth, and ellipticity of polarization of each point of Fourier spectrum can be determined from the next relations[21]

$$U_x(\mu, \nu) = \frac{A}{i\lambda f} \int_{-\infty}^{+\infty} E_x(x, y) \exp\left[-i\frac{2\pi}{\lambda f}(x\mu + y\nu)\mathrm{d}x\,\mathrm{d}y\right]; \quad (7)$$

$$U_y(\mu, \nu) = \frac{A}{i\lambda f} \int_{-\infty}^{+\infty} E_y(x, y) \exp\left[-i\frac{2\pi}{\lambda f}(x\mu + y\nu)\mathrm{d}x\,\mathrm{d}y\right]. \quad (8)$$

Here U_x, U_y—amplitudes in the points of Fourier images of distributions of amplitudes of polarization-inhomogeneous field $E_x(\rho, \delta, \theta)$ and $E_y(\rho, \delta, \theta)$ in boundary (near-surface) zone. Here $\nu = (x/\lambda f)$ and $\mu = (y/\lambda f)$—spatial frequencies, λ—laser radiation wavelength; and f—focal distance of microobjective.

By analogy with Eqs. (4)–(6) polarization maps $[\alpha^*(\mu, \nu), \beta^*(\mu, \nu)]$ of polarization-inhomogeneous Fourier images of human skin were determined in accordance with the following relations

$$\alpha^*(\mu, \nu) = 0.5 \arcsin\left[\frac{\sin 2\Theta(\mu, \nu)}{\cos \chi(\mu, \nu)}\right]; \quad (9)$$

$$\beta^*(\mu, \nu) = 0.5 \arctan\left[\frac{\sin \chi(\mu, \nu)}{\cos 2\Theta(\mu, \nu)}\right], \quad (10)$$

where χ—phase shift between the orthogonal component of laser field amplitude U_x, U_y in Fourier plane, $\Theta = \arctan(U_y/U_x)$.

Comparative analysis of the structure of polarization-inhomogeneous object fields of human skin in different registration zones {boundary plane [Eqs. (4) and (5)—*in vitro*] and Fourier plane [Eqs. (9) and (10)—*in vivo*]} reveals the dependence between the distributions of polarization azimuths (α, α^*) and ellipticities (β, β^*) values and anisotropy parameters (ρ, φ, θ) of human skin. It is known[12,14,15] that oncological changes of biological tissues accompanied by increasing of optical anisotropy ($\varphi \uparrow$, $\theta \uparrow$) due to destructive processes of neoplasms formation. Optical "indicators" of such changes are the transformation of the distribution of values of polarization parameters of object laser fields, transformed by human skin with various types of pathology. Quantitatively and objectively, these processes *in vivo* can be assessed by monitoring changes of a set of statistical moments of the 1st to 4th order, describing the distribution of values of polarization azimuth α^* and ellipticity β^* in Fourier plane.

3 Experimental Results and Discussion

The most important monitoring of human skin pathological changes is on early, precancerous stages. Therefore, in this paper we have performed the following steps:

- at the first stage the possibility of finding a set of criteria (statistical moments of 1st to 4th order, describing distribution of values of azimuth and ellipticity of polarization in the Fourier plane) of noninvasive optical diagnostics of human skin during the differentiation of its conditions was examined;
- at the second stage such data were compared with the decisions of histological studies ("gold standard") of biopsy samples of benign and precancerous skin formations;
- at the third stage sensitivity, specificity, and accuracy of the method of Fourier polarimetry were determined.

3.1 *Brief Characteristics of the Investigation Objects and Experimental Setup of Fourier Polarimetry*

As the objects of optical (*in vivo*) and histological (*in vitro*) investigations, we chose two types of human skin pathological states

- patients with the benign (sebaceous adenoma—group 1 to 47 patients) skin changes. A biopsy of tumors was taken from the neck and trunk of patients.

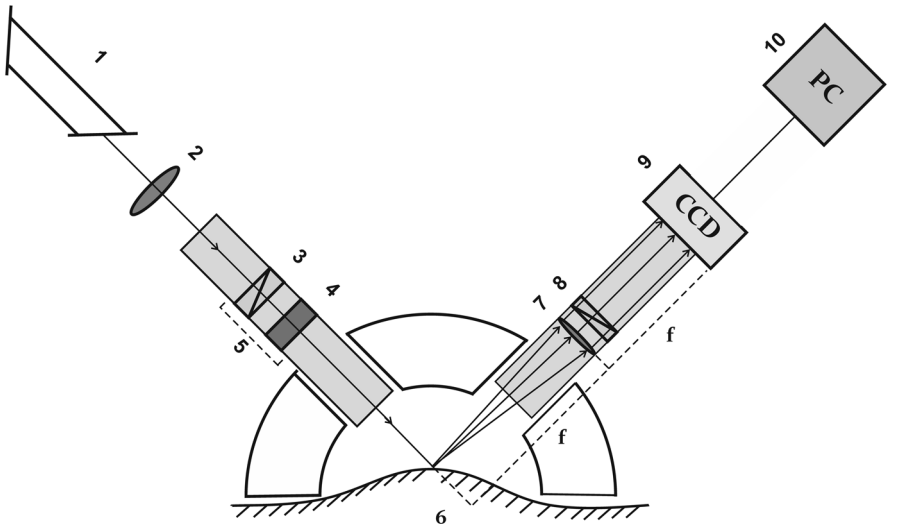

Fig. 1 An optical diagram of Fourier–Stokes polarimeter, where 1—He-–Ne laser, 2—collimator; 3, 8—polarizers; 4—a stationary quarter-wave plate; 5—optical fiber; 6—skin surface; 7—strain-free objective; 9—step motor, 10—CCD camera; 11—a personal computer.

- patients with the precancer (keratoma—group 2 to 47 patients) skin changes. A biopsy of abnormal skin was taken from the shoulders and legs of patients.

Optical investigations of pathologically changed skin areas were made in the following experimental arrangement. Figure 1 shows an optical scheme of Fourier–Stokes polarimeter. Illumination was performed with an expanded beam of a He–Ne laser ($\lambda = 0.6328$ μm, $G = 5.0$ mW). The polarization illuminator consists of the polarizer 3, quarter-wave plate 4, and single-mode optical fiber 5.

Strain-free objective 7 (Nikon CFI Achromat P, working distance—30 mm, aperture—0.1, magnification—4×) is placed at the focal length from the skin surface six. Such a scheme provides the illumination of the human skin area ($S = 20$ mm^2) and forms the Fourier spectrum of scattered radiation in the plane of CCD-camera 10 [The Imaging Source DMK 41AU02.AS, monochrome $1/2''$ CCD, Sony ICX205AL (progressive scan); resolution—1280×960; light sensitive area size—7600×6200 μm; sensitivity—0.05 lx; dynamic range—8 bit; SNR—9 bit, deviation of photosensitive characteristics from linear no more than 5%].

The analysis of polarization structure of Fourier spectra of radiation scattered by skin was performed by means of polarizer–analyzer 8. By turning with the help of step 9 the analyzer axis at an angle Θ within 0 deg–180 deg the arrays of minimal and maximal intensity levels $I_{\min}(m \times n)$; $I_{\max}(m \times n)$ were determined for every pixel $(m \times n)$ of CCD-camera, as well as the rotation angles $\Theta(m \times n)[I(m \times n) \equiv \min]$ corresponding to them. Further, the coordinate distributions (polarization maps) of polarization azimuths and ellipticities of the field of reflected radiation were calculated using the following ratios[20]

$$\alpha^*(m \times n) = \Theta(I \equiv \min) - \frac{\pi}{2};$$
$$\beta^*(m \times n) = \operatorname{arctg}\left(\frac{I_{\min}}{I_{\max}}\right). \tag{11}$$

In order to obtain reproducible (valid) experimental polarization distributions Eq. (11) we have used probing laser beam with right circular polarization for adenoma and keratoma illumination. Illustrative photos of typical abnormal skin are shown in Fig. 2. Under these conditions, the value of polarization azimuth α^* and ellipticity β^* in the points of Fourier spectrum appears to be azimuthally-invariant in relation to the direction of collagen fibrils packing and the orientation of epidermis plates.

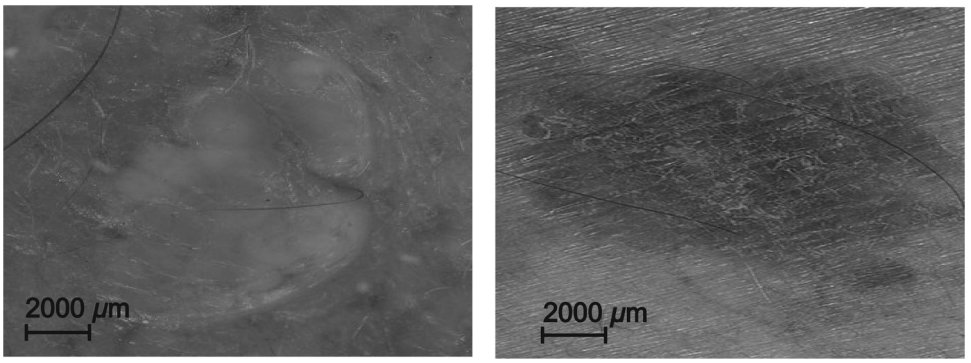

(a) (b)

Fig. 2 Photos of typical abnormal human skin areas with adenoma (a) and keratoma (b).

3.2 *Polarization-Inhomogeneous Fourier Spectra of Object Field of Human Skin*

Figures 3 and 4 shows the central parts (800×600 μm) of polarization maps of azimuths $\alpha^*(\mu,\nu)$ [Figs. 3(a) and 3(b)], and ellipticities $\beta^*(\mu,\nu)$ [Figs. 4(a) and 4(b)] and the corresponding histograms of their values [Figs. 3(c), 3(d), 4(c), and 4(d)] of the Fourier spectra of reflected radiation by patient's skin of group 1 (b, d) and group 2 (a, c).

The obtained data show that

1. Fourier spectra of laser radiation reflected by skin are polarization-inhomogeneous [Figs. 3(a), 3(b), 4(a), and 4(b)].
2. Histograms of values of polarization azimuths and ellipticities of Fourier spectra of reflected radiation are characterized by the maximal possible range of changing ($\alpha = -90$ deg $\div 90$ deg and $\beta = -45$ deg $\div 45$ deg) [Figs. 3(c), 3(d), 4(c), and 4(d)].

Provided experimental results confirm the influence of optical anisotropy of human skin, as it has been predicted in the model [Eqs. (1)–(10)], on the formation of polarization structure of Fourier spectra of reflected radiation.

It has been revealed that the polarization structure of Fourier spectra is different depending on the pathology type (benign-malignant states) of skin. In the case of keratoma (group 2), the dispersion of polarization parameters values of Fourier spectrum of reflected radiation is less than for adenoma (group 1) [Figs. 3(d) and 4(d)]. Such fact, in our opinion, can be connected with the destructive changes of birefringent structures of human skin.[2,7,9,11,16]

3.3 *Statistical Analysis of Polarization-Inhomogeneous Fourier Spectra of the Object Field of Human Skin*

For the purpose of objective (quantitative) estimation of the distributions $\alpha^*(\mu,\nu)$ and $\beta^*(\mu,\nu)$ we have used a statistic approach. Statistical moments of the first (R_1), the second (R_2), the third (R_3), and the fourth (R_4) orders were calculated by the following algorithms:

$$R_1 = \frac{1}{P}\sum_{j=1}^{P}(|q|)_j; \quad R_2 = \sqrt{\frac{1}{P}\sum_{j=1}^{P}[(q-R_1)^2]_j};$$
$$R_3 = \frac{1}{R_2^3}\frac{1}{P}\sum_{j=1}^{P}[(q-R_1)^3]_j; \quad R_4 = \frac{1}{R_2^4}\frac{1}{P}\sum_{j=1}^{P}[(q-R_1)^4]_j, \tag{12}$$

where $P = 1280 \times 960$—amount of pixels of CCD-camera; $q \equiv (\alpha^*, \beta^*)$.

The methodology of differential diagnostics of skin pathology *in vivo* includes the following steps:[22–24]

1. Formation of representative samples of groups of patients. For this purpose

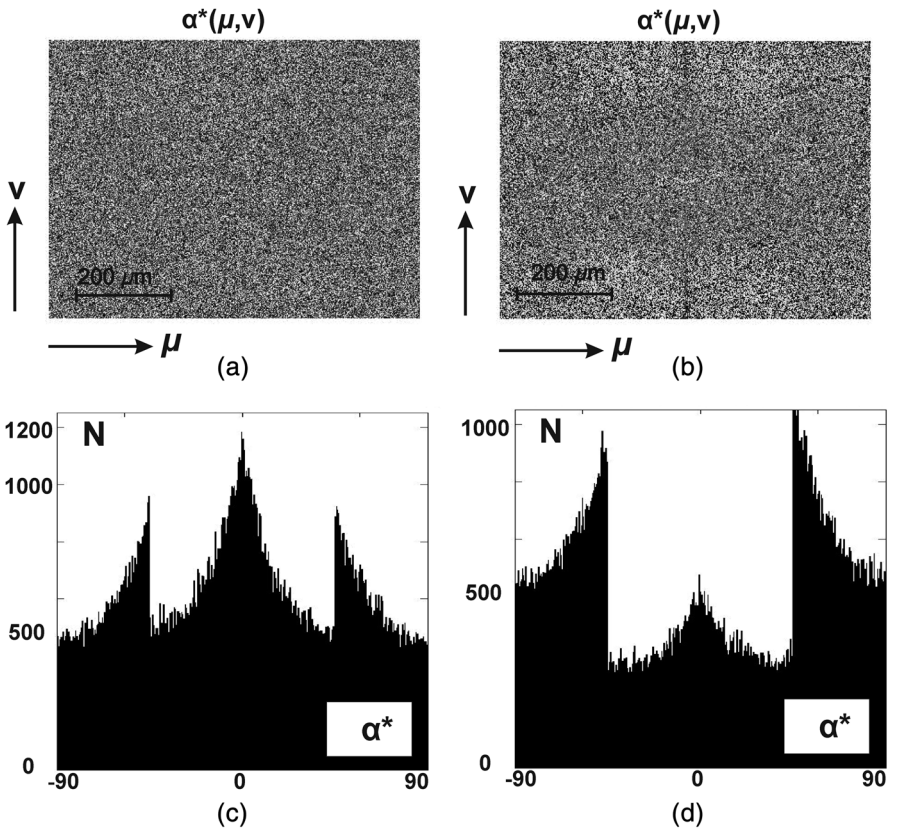

Fig. 3 (a) and (b) Polarization maps $\alpha^*(\mu,\nu)$ and the (c) and (d) histograms of distributions $N(\alpha^*)$ of laser images of (a) and (c) adenoma and (b) and (d) keratoma of human skin in Fourier plane.

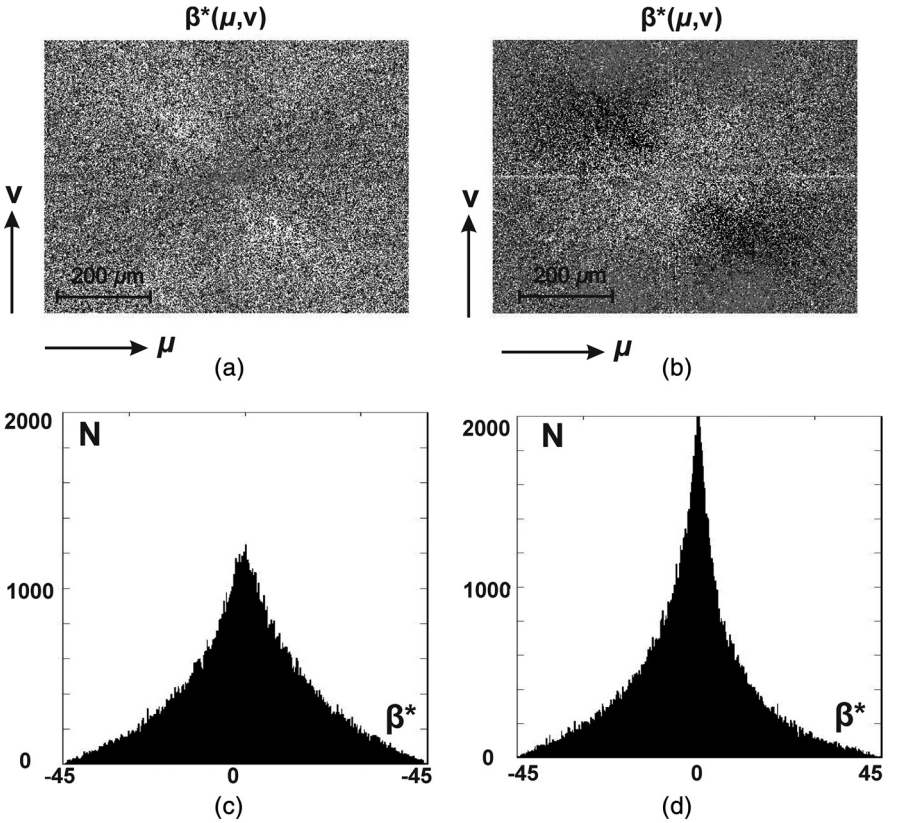

Fig. 4 (a) and (b) Polarization maps $\beta^*(\mu,\nu)$ and the (c) and (d) histograms of distributions $N(\beta^*)$ of laser images of (a) and (c) adenoma and (b) and (d) keratoma of human skin in Fourier plane.

- for each patient from group 1 and group 2 we measured the distributions of values of polarization parameters [Eq. (11), Figs. 3 and 4] of Fourier spectra of reflected laser radiation;
- for each distribution of values of $\alpha^*(\mu,\nu)$ and $\beta^*(\mu,\nu)$ we calculated the statistical moments of the 1st to 4th orders $R_{i=1;2;3;4}(\alpha^*)$ and $R_{i=1;2;3;4}(\beta^*)$ [Eq. (12)];
- for a specified significance level ($p = 0.05$) we calculated the statistical power by using of z-test (Fisher's z-criterion);
- above-mentioned steps were in progress for each of the eight obtained sets of values of statistical moments $R_i(\alpha^*)$ I $R_i(\beta^*)$ until the range of statistical power reached 95%;
- as a result we have obtained the statistically reliable number of patients within the groups 1 and 2 $n = 47$.

2. The differentiation between the group 1 and group 2 was performed by using of the following methodology:

- within each set of values of statistical moments $R_{i=1;2;3;4}(q)$ we determined the average value $\bar{R}_{i=1;2;3;4}(q)$ and standard deviation $\sigma_{i=1;2;3;4}(q)$;
- differences between the statistical sets $R_{i=1;2;3;4}(q)$ were significant in the case when the average value $\bar{R}_{i=1;2;3;4}(q)$ within the group 1 didn't overlap with the range $1.96 \times \sigma_{i=1;2;3;4}(q)$ (this provides 95% of confidence interval) within group 2 and vice versa (see Table 1).

3. For the possible clinical application of such method traditional for probative medicine operational characteristics: sensitivity [$\mathrm{Se} = (a/a+b)100\%$], specificity [$\mathrm{Sp} = (c/c+d)100\%$], and balanced accuracy ($\mathrm{Ac} = [(\mathrm{Se}+\mathrm{Sp})/2]$), where a and b are the number of correct and wrong diagnoses within group 2; c and d—the same within group 1 were determined. For this purpose

- within both groups of patients for the distributions of values of each statistical moments $R_{i=1;2;3;4}(q)$ we

Table 1 Statistical moments of the 1st to 4th orders of the distributions of polarization azimuths [$\alpha^*(\mu,\nu)$] and ellipticities [$\beta^*(\mu,\nu)$] of human skin Fourier spectra.

	$\alpha^*(\mu,\nu)$		$\beta^*(\mu,\nu)$	
	Group 1	Group 2	Group 1	Group 2
Parameters	$R_i \pm 1.96\sigma_i$		$R_i \pm 1.96\sigma_i$	
R_1	0.14 ± 0.008	0.11 ± 0.007	0.08 ± 0.005	0.06 ± 0.004
R_2	0.31 ± 0.025	0.25 ± 0.017	0.13 ± 0.009	0.11 ± 0.007
R_3	$1.79 \pm 0{,}12$	$0.83 \pm 0{,}13$	0.57 ± 0.032	0.88 ± 0.061
R_4	1.47 ± 0.11	2.26 ± 0.16	0.86 ± 0.057	1.27 ± 0.09

Table 2 Operational characteristics of the method of Fourier polarimetry of reflected by skin laser radiation.

Parameters, %			$\alpha^*(\mu,\nu)$			$\beta^*(\mu,\nu)$
Se	R_1	62	$a=29;\ b=18$	R_1	57	$a=27;\ b=20$
	R_2	70	$a=33;\ b=14$	R_2	66	$a=31;\ b=16$
	R_3	**96**	$a=45;\ b=2$	R_3	87	$a=41;\ b=6$
	R_4	89	$a=42;\ b=5$	R_4	**92**	$a=43;\ b=4$
Sp	R_1	68	$c=32;\ d=15$	R_1	64	$c=30;\ d=17$
	R_2	74	$c=35;\ d=12$	R_2	70	$c=33;\ d=14$
	R_3	**94**	$c=44;\ d=3$	R_3	81	$c=38;\ d=9$
	R_4	87	$c=41;\ d=6$	R_4	**86**	$c=40;\ d=7$
Ac	R_1	65	$a=29;\ b=18;\ c=22;\ d=15$	R_1	62	$a=27;\ b=20;c=30;\ d=17$
	R_2	72	$a=33;\ b=14;\ c=35;\ d=12$	R_2	68	$a=31;\ b=16;\ c=33;\ d=14$
	R_3	**95**	$a=42;\ b=5;\ c=44;\ d=3$	R_3	84	$a=41;\ b=6;\ c=38;\ d=9$
	R_4	88	$a=42;\ b=5;\ c=41;\ d=6$	R_4	**89**	$a=43;\ b=4;\ c=40;\ d=7$

chose cutoff of 3σ (99.72% of all possible values of changes of R_i);

- sequentially, we determined the number of "false negative" (b) and "false positive" (d) conclusions;
- for each of statistical moments $R_{i=1;2;3;4}(q)$ we calculated the values of sensitivity Se, specificity Sp, and balanced accuracy Ac of diagnostical test of Fourier polarimetry of laser radiation reflected by human skin (see Table 2);
- from the obtained data $\{\mathrm{Se}[R_i(q)],\ \mathrm{Sp}[R_i(q)]\ \mathrm{IAc}[R_i(q)]\}$ we chose the maximal values of operational characteristics—highlighted in bold in Table 2.

Therefore, operational characteristics of the method of Fourier polarimetry of reflected by skin laser radiation in the tasks of differentiation of benign and malignant states reached the excellent quality of diagnostic test—$Ac(\alpha^*,\beta^*)=92\%-96\%$.[22]

4 Conclusions

1. The distributions of polarization parameters of reflected by skin laser radiation (adenoma and keratoma) in Fourier plane were measured.
2. The set of statistical (statistical moments of the 1st to 4th orders) parameters characterizing the distributions of azimuths and ellipticities of laser radiation in Fourier plane were calculated.
3. It was shown that the most sensitive for diagnostics and differentiations of pathological changes of human skin appeared to be the following statistical moments: of the 3rd order, which characterized the skewness of the distribution of polarization azimuth values, and of the 4th order, which characterized the kurtosis of the distribution of polarization ellipticities values of polarization-inhomogeneous Fourier spectra of human skin.
4. The operational characteristics of the method of Fourier polarimetry of laser radiation reflected by human skin were determined. The excellent quality of diagnostic test of such optical method in the task of differentiation of benign and malignant states was achieved.

References

1. L. E. Preuss and A. E. Profio, "Optical properties of mammalian tissue: introduction by the feature editors," *Appl. Opt.* **28**, 2207–2207 (1989).
2. W. F. Cheong, S. A. Prahl, and A. J. Welch, "A review of the optical properties of biological tissues," *IEEE J. Quantum Electron.* **26**, 2166–2185 (1990).
3. S. A. Prahl et al., "A Monte Carlo model of light propagation in tissue," in *SPIE Proc. of Dosimetry of Laser Radiation in Medicine and Biology*, Vol. **IS 5**, pp. 102–111 (1989).
4. M. R. Ostermeyer et al., "Nearfield polarization effects on light propagation in random media," *Trends in Optics and Photonics: Biomedical Optical Spectroscopy and Diagnostics*, Vol. 3, pp. 20–26 (1996).
5. P. Bruscaglioni, G. Zaccanti, and Q. Wei, "Transmission of a pulsed polarized light beam through thick turbid media: numerical results," *Appl. Opt.* **32**, 6142–6150 (1993).
6. V. Sankaran et al., "Comparison of polarized-light propagation in biological tissue and phantoms," *Opt. Lett.* **24**, 1044–1046 (1999).
7. M. C. Pierce et al., "Birefringence measurements in human skin using polarization-sensitive optical coherence tomography," *J. Biomed. Opt.* **9**, 287–291 (2004).
8. J. F. de Boer et al., "Two-dimensional birefringence imaging in biological tissue by polarization-sensitive optical coherence tomography," *Opt. Lett.* **22**, 934–936 (1997).
9. C. E. Saxer et al., "High-speed fiber based polarization-sensitive optical coherence tomography of in vivo human skin," *Opt. Lett.* **25**, 1355–1357 (2000).
10. J. F. de Boer and T. E. Milner, "Review of polarization sensitive optical coherence tomography and Stokes vector determination," *J. Biomed. Opt.* **7**, 359–371 (2002).

11. Y. Yasuno et al., "Birefringence imaging of human skin by polarization-sensitive spectral interferometric optical coherence tomography," *Opt. Lett.* **27**, 1803–1805 (2002).
12. O. V. Angelsky et al., "Statistical, correlation, and topological approaches in diagnostics of the structure and physiological state of birefringent biological tissues," in *Handbook of Photonics for Biomedical Science*, V. V. Tuchin, Ed., pp. 283–322, CRC Press, Taylor & Francis group, New York (2010).
13. A. G. Ushenko, "Polarization structure of biospeckles and the depolarization of laser radiation," *Opt. Spectrosc.* **89**, 597–600 (2000).
14. Yu. A. Ushenko, O. V. Dubolazov, and A. O. Karachevtsev, "Statistical structure of skin derma Mueller matrix images in the process of cancer changes," *Opt. Mem. Neural Networks* **20**, 145-154 (2011).
15. A. G. Ushenko et al., "Evolution of statistic moments of 2D- distributions of biological liquid crystal netmueller matrix elements in the process of their birefringent structure changes," *Adv. Opt. Technol.* **2010**, 423145 (2010).
16. Y. A. Ushenko, A. P. Peresunko, and B. Adel Baku, "A new method of Mueller-Matrix diagnostics and differentiation of early oncological changes of the skin derma," *Adv. Opt. Technol.* **2010**, 952423 (2010).
17. O. V. Angelsky et al., "Optical measurements: polarization and coherence of light fields," in *Modern Metrology Concerns*, L. Cocco, ed., pp. 263–316, InTech, Croatia, Europe (2012).
18. Y. A. Ushenko et al., "Diagnostics of structure and physiological state of birefringent biological tissues: statistical, correlation and topological approaches," in *Handbook of Coherent-Domain Optical Methods*, p. 107, Springer Science+Business Media, New York (2013).
19. Y. O. Ushenko et al., "Complex degree of mutual anisotropy of biological liquid crystals nets," *Opt. Eng.* **50**, 039001 (2011).
20. A. O. Karachevtsev, "Fourier Stokes-polarimetry of biological layers polycrystalline networks," *Semicond. Phys. Quantum Electron. Optoelectron.* **15**(3), 252–268 (2012).
21. J. W. Goodman, "Statistical properties of laser speckle patterns," in *Laser Speckle and Related Phenomena*, J. C. Dainty, ed. pp. 9–75, Springer-Verlag, Berlin (1975).
22. L. D. Cassidy, "Basic concepts of statistical analysis for surgical research," *J. Surg. Res.* **128**, 199–206 (2005).
23. C. S. Davis, *Statistical Methods of the Analysis of Repeated Measurements*, pp. 744, Springer-Verlag, New York (2002).
24. A. Petrie and B. Sabin, *Medical Statistics at a Glance*, pp. 157, Blackwell Publishing Ltd., Oxford, UK (2005).

Alexander G. Ushenko is a doctor of physics and mathematics, professor and head of the Department of Optics and Spectroscopy at Chernivtsi National University. He is an author of over 150 scientific articles, 14 monographs, and 37 patents. His areas of expertise include polarimetry of biological tissues and fluids and autofluorescence polarimetry.

Alexander V. Dubolazov received his PhD in biomedical optics. He is an associate professor in the Department of Optics and Spectroscopy in Chernivtsi National University. He is an author of over 50 scientific articles, 14 monographs, and 4 patents. His area of expertise includes Mueller-matrix polarimetry of biological tissues and fluids.

Vladimir A. Ushenko received his PhD in biomedical optics. He is an assistant professor at the Correlation Optics Department in Chernivtsi National University. He is an author of over 50 scientific articles and 3 patents. His area of expertise includes Mueller-matrix polarimetry of biological tissues and fluids.

Olga Y. Novakovskaya received her PhD in biomedical optics. She is an assistant professor at the Department of Medical Physics and Biological Informatics in Bukovinian State Medical University. She is an author over 30 scientific articles and 2 patents. Her area of expertise includes Mueller-matrix polarimetry of biological tissues and fluids.